

Multiple unitary-pulses for coherent-control of tunnelling and decoherence

LUIS G. C. REGO[‡], SABAS G. ABUABARA[†]
and VICTOR S. BATISTA^{*†}

[†]Department of Chemistry, Yale University, PO Box 208107
New Haven, CT 06520-8107, USA

[‡]Department of Physics, Universidade Federal de Santa Catarina
Florianopolis, SC 88040-900, Brazil

(Received 16 March 2007; in final form 3 July 2007)

This paper investigates the feasibility of using sequences of unitary pulses for achieving coherent-control of quantum dynamical phenomena, including quantum control of electron tunnelling in archetype model systems and control of decoherence in a quantum dot system coupled to a thermal bath. The proposed dynamical decoupling scenario is based on the repetitive application of 2π pulses, affecting the interference phenomena between wave-packet components. The pulses affect the overall relaxation dynamics without collapsing the coherent-quantum evolution of the system. It is shown that both bound-to-bound state tunnelling and bound-to-continuum tunnelling processes can be inhibited and eventually halted by sufficiently frequent pulse fields that exchange energy with the system but do not affect the potential energy tunnelling barriers. Furthermore, the proposed quantum-control scenario is demonstrated as applied to manipulating the electronic quantum dynamics in a quantum dot coupled to a free standing quasi two-dimensional phonon cavity. The reported results are therefore particularly relevant to the understanding of coherent optical manipulation of electronic excitations in semiconductor devices where performance is limited by quantum tunnelling and decoherence.

1. Introduction

The possibility of engineering semiconductor devices at the nano and micro scales has created the conditions for testing fundamental aspects of quantum theory otherwise difficult to probe in natural atomic size systems. Particularly, quantum dot (QD) structures are recognized as physical realizations of artificial atoms and molecules whose properties (e.g. structural and transport) can be engineered for

*Corresponding author. Email: victor.batista@yale.edu

specific applications and modulated in the presence of external fields [1–3]. In fact, coupled arrays of QDs have already been proposed to create charge or spin qubit gates [4–6], and quantum memory units [7]. However, an outstanding challenge is the development of efficient methods for controlling decoherence. Control of tunnelling dynamics has also attracted much attention [8–16] due to the potential application of these effects in quantum computation [17–19]. In particular, the study of dynamic localization and coherent destruction of quantum tunnelling has become a subject of great research interest [20–26]. However, efficient methods for coherent manipulation of decoherence and quantum tunnelling dynamics have yet to be established. This paper investigates a simple coherent-control method, based on sequences of unitary pulses, as applied to simulating quantum control of electronic tunnelling and electronic decoherence.

In recent work, we have investigated a coherent-control technique for optical manipulation of electronic relaxation in functionalized semiconductor nanostructures [27, 28]. The method involves using deterministic [27], or stochastic [28], sequences of unitary pulses that affect the interference phenomena between wave-packet components and consequently the overall relaxation dynamics, without collapsing the coherent-quantum evolution of the systems. This paper further investigates such a coherent-control technique as applied to optical manipulation of tunnelling dynamics in general, including bound-to-bound state tunnelling and bound-to-continuum tunnelling processes as well as coherent-control of electronic decoherence in a model quantum dot coupled to a phonon cavity consisting of a suspended semiconductor nanoelectromechanical structure.

In analogy to our previous studies, the reported computational results show that the frequent application of unitary pulses affects the overall quantum dynamics by altering the interference phenomena between quantum states, inducing coherent energy exchange between the system and the perturbational field. The resulting control of decoherence is related to the Zeno effect [29] in a broad sense, although with significant differences. While in our method the interaction with an external perturbation does not collapse the coherent unitary propagation, other perturbative schemes could delay (Zeno effect) or accelerate (anti-Zeno effect) the decoherence process [30]. Recently, unifying approaches, based on an adiabatic theorem [31] or considering the quantum measurement theory in detail [32], have been proposed to explain the various forms of Zeno effects, produced by non-unitary pulses (measurements), unitary pulses (dynamical decoupling) or continuous strong coupling. In addition, our coherent-control mechanism differs from other dynamical localization schemes that use external driving fields to modulate the potential energy landscape [21, 22, 33].

The paper is organized as follows. First, section 2 reviews the coherent control scenario based on sequences of multiple unitary pulses. Section 3 investigates the implementation of the coherent-control scenario, introduced in section 2, as applied to manipulating bound-to-bound state tunnelling and bound-to-continuum tunnelling processes. Section 4 then investigates coherent control of electronic dynamics in a model quantum dot–nanoelectromechanical system. Finally, section 5 summarizes and concludes.

2. Quantum control with sequences of unitary pulses

The coherent-control scenario implemented in this paper constitutes a generalization of the recently reported quantum-control scheme based on deterministic 2π unitary pulses [34]. This optical control method is a form of dynamical decoupling, analogous to other approaches for modulating quantum relaxation dynamics based on sequences of frequent unitary pulses [35–38]. These methods thus preserve the coherent nature of the unitary evolution which is expected to be particularly useful for applications in quantum information processing.

The essence of the method, proposed originally in [35], involves coupling a target state $|1\rangle$ with an auxiliary state $|2\rangle$ by using the optical pulse

$$\hat{U}^\Phi = \cos\left[\frac{\Gamma\tau}{2}\right](|1\rangle\langle 1| + |2\rangle\langle 2|) - i \sin\left[\frac{\Gamma\tau}{2}\right](|1\rangle\langle 2| + |2\rangle\langle 1|), \quad (1)$$

where $\Phi = \Gamma\tau/2$ is the phase-shift, defined by the product of the optical Rabi frequency Γ and a random effective pulse duration τ (duration of the resonance between Γ and the desired optical transition). In the particular case of $\Gamma\tau = 2\pi$, the time-evolution operator becomes the deterministic 2π pulse, $\hat{U}_{2\times 2}^{2\pi} = -|1\rangle\langle 1| - |2\rangle\langle 2|$ inducing only a π phase-shift $|\Psi_{2\pi}\rangle = \hat{U}^{2\pi}|\Psi\rangle$ in the time-evolved wave-packet component corresponding to state $|1\rangle$ so long as $\langle 2|\Psi\rangle = 0$.

In previous applications, this quantum-control scheme has been applied for manipulation of superexchange hole-tunnelling dynamics in functionalized TiO_2 nanostructures [28, 34], where $|1\rangle$ was an electronic state of an adsorbate molecule and $|2\rangle$ was an auxiliary state of the same adsorbate, also off-resonant to the semiconductor valence and conduction bands. The current studies extend the range of applications to studies of tunnelling dynamics in general model systems and decoherence in quantum dots coupled to a phonon cavity. In all of these applications, it is assumed that the colour of the perturbational pulses can be tuned to be resonant with the $|1\rangle \rightarrow |2\rangle$ transition, without significantly interacting with any of the other $N-2$ states within the N -level system. The full time evolution operator is thus the sum $\mathbf{I}_{(N-2)\times(N-2)} + \hat{U}_{2\times 2}^{2\pi} = \mathbf{I}_{N\times N} - \mathbf{I}_{2\times 2} + \hat{U}_{2\times 2}^{2\pi}$. Furthermore, for $\Psi_0 \equiv |\Psi(t=0)\rangle$, the 2π pulse time-evolution operator can be numerically implemented as the unitary operator, $\hat{U}^{2\pi} = \mathbf{I} - 2|\Psi_0\rangle\langle\Psi_0|/\langle\Psi_0|\Psi_0\rangle = \mathbf{I} - 2|\Psi_0\rangle\langle\Psi_0|$, as reported in previous work [34], where \mathbf{I} is the identity matrix and $\langle\Psi_0|\Psi_0\rangle = 1$.

3. Coherent-control of tunnelling dynamics

This section illustrates the quantum-control scenario, introduced in section 2, as applied to two archetype model systems. The first model involves an electron tunnelling through the quartic double-well potential described by the Hamiltonian, $\hat{H} = (\hat{p}^2/2m_e) + V(\hat{x})$, where $V(\hat{x}) = -\alpha\hat{x}^2 + \beta\hat{x}^4$, with $\alpha = 0.5$ au and $\beta = 0.0461$ au (i.e. an oscillating system, see figure 1(a)). The second model involves an electron tunnelling through a barrier from a quasi-bound state into a continuum (i.e. a truly decaying system). The potential energy barrier is defined according to the

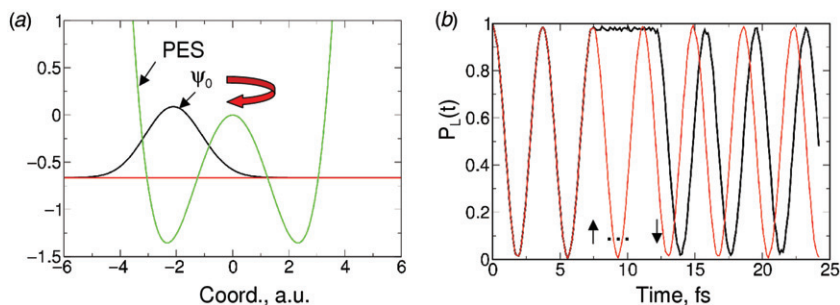


Figure 1. (a) Quartic double-well potential (green) and initial state (black). (b) Probability of the system to be found in the left well, as a function of time, without any external perturbation (red) and perturbed by π phase unitary pulses (black) in the time interval indicated by the arrows. (The colour version of this figure is included in the online version of the journal.)

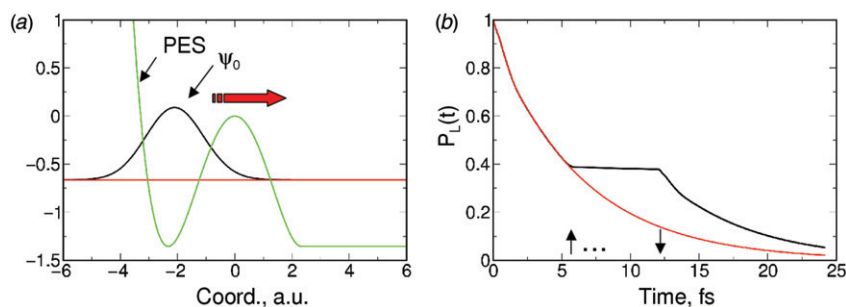


Figure 2. (a) Potential energy barrier defined in the text (green) and initial state (black). (b) Probability of the system to be found in the left well, as a function of time, without any external perturbation (red) and perturbed by π phase unitary pulses (black) in the time interval indicated by the arrows. (The colour version of this figure is included in the online version of the journal.)

quartic potential, for $x \leq x_e$ where x_e is the equilibrium position on the rhs of the barrier, and constant otherwise (see figure 2(a)). Wave-packet propagations are based on the standard grid-based implementation of the split operator Fourier transform (SOFT) method [39–41] which can be applied in dynamically adaptive coherent-state representations according to the matching-pursuit (MP)/SOFT approach [42–48] in studies of quantum dynamics in multidimensional model systems.

Figure 1(b) shows the time-dependent probability of finding the electron on the left side of the tunnelling barrier during the first 25 fs of dynamics. A comparison of the underlying tunnelling dynamics, in the absence of perturbational pulses (red line), or perturbed (black line) by a sequence of 2π unitary pulses in the time-window indicated by the arrows, is presented. Here, each pulse adds a phase shift to the component of the time-dependent wavefunction corresponding to the initial state. The phase manipulation could plausibly be effected by a sequence of ultrashort

2π pulses coupling each of the two lowest energy levels of the double-well potential surface, respectively, to two distinct levels of an auxiliary surface (one symmetric, one antisymmetric to obey parity selection rules resulting from considering the dipole operator). The simulation results for this case, presented in figure 1, clearly demonstrate that a regular sequence of π phase kicks applied to a component of the time-evolved wavepacket can inhibit tunnelling dynamics and yet preserve coherence, since the coherent tunnelling dynamics continues after termination of the pulse sequence. Similar results can be obtained with generalizations of this scheme in which both the intervals between pulses and the values of the phase-shifts are randomized [28], so long as the average time-interval between pulses is much shorter than the tunnelling period. Note that coherent-control of tunnelling dynamics is accomplished simply by manipulating the phase of a wavepacket component through an interaction that is instantaneous compared to the timescales determined by the potential energy barrier, but without affecting the potential energy surface. However, the net-effect is similar to the phenomenon called *coherent destruction of tunnelling* [26], first reported by Grossman and co-workers [21], where the (usually monochromatic) oscillatory term in the Hamiltonian modulates the potential barrier and may inhibit tunnelling or localize the wavepacket [49].

The coherent control scenario demonstrated for the quartic double-well potential is also effective at hindering tunnelling from a quasi-bound state into a continuum. Figure 2(b), shows the time-dependent probability of finding an electron in the initial quasi-bound state on the left side of the tunnelling barrier into a continuum during the first 25 fs of dynamics. A comparison of the underlying tunnelling dynamics, in the absence of perturbational pulses (red line), or when perturbed (black line) by a sequence of 2π unitary pulses in the time-window indicated by the arrows, is presented. In analogy with the previous example, each pulse adds a phase shift to the component of the time-dependent wavefunction corresponding to the initial state. The simulation clearly demonstrates that spontaneous decay by tunnelling to a continuum can be significantly slowed down while the train of 2π pulses is applied and re-established upon termination of the pulse sequence.

An interesting observation can be made by comparing the results of tunnelling dynamics into a continuum (figure 2) to the corresponding results obtained for the double-well potential (figure 1). Note that in the absence of the wall on the rhs of the double-well potential the first tunnelling event becomes significantly slower, stretching the time it takes for reaching 50% of population decay from less than 1 fs in the double-well potential to more than 5 fs when tunnelling into a continuum. In the dynamics picture, this indicates that tunnelling requires interference between wavepacket components on both sides of the barrier. The underlying interference phenomena is more effective in the bound-to-bound state tunnelling process than in the bound-to-continuum tunnelling dynamics simply because the wavepacket components that tunnel into the continuum continue moving outbound. Therefore, the bound-to-continuum tunnelling is slower than the bound-to-bound tunnelling process. Analogously, the unitary pulses affect the interference phenomena between the decaying state and the rest of the states in the system, slowing down the underlying tunnelling dynamics.

4. Coherent control of decoherence in a model quantum dot-nanoelectromechanical system

A new exciting possibility for both implementing and investigating coherent phenomena in semiconductors is the combination of quantum dot systems with suspended nanostructures [50–54]. An immediate consequence of such a combination is the improved isolation of the electronic quantum system from the bulk of the sample, that can allow for longer lived coherent quantum states. Furthermore, phonon cavities can also be envisaged as the solid state analogue of quantum electrodynamic (QED) cavities [55]. Nonetheless, since the electron–phonon interaction can be controlled in such devices, new physics can be expected to develop. For instance, it has been shown that suspended nanoelectromechanical structures can exhibit a rich quantum chaotic behaviour [56, 57].

In this section we make use of a free standing QD–phonon cavity structure to demonstrate that the dynamics of a non-trivial quantum system can be coherently manipulated through a train of unitary 2π pulses even in the presence of a thermal bath. The physical model consists of a circular QD (electronic system) located at the surface of a free standing quasi two-dimensional silicon membrane (see figure 3). The proposed suspended heterostructure comprises typical nanomachining technology [52], including the QD that can be produced by selectively doping a circular area at the surface of the silicon plate or by means of suspended metallic gates [51]; a finer detailed description of the system will be provided in the following.

In the following we solve the time-dependent Schrödinger equation by direct diagonalization of the compound system, i.e. the QD coupled with the phonon cavity. The Hamiltonian of the system can be written as

$$\begin{aligned} \hat{H} &= \hat{H}_{\text{el}} + \hat{H}_{\text{ph}} + \hat{H}_{\text{el-ph}} \\ &= \sum_{\kappa} E_{\kappa} b_{\kappa}^{\dagger} b_{\kappa} + \sum_{\alpha} \left(\hat{n}_{\alpha} + \frac{1}{2} \right) \hbar \omega_{\alpha} + \sum_{\alpha \kappa \kappa'} V_{\kappa' \alpha \kappa} b_{\kappa'}^{\dagger} [a_{\alpha}^{\dagger} + a_{\alpha}] b_{\kappa}, \end{aligned} \quad (2)$$

including the electron and phonon ensemble Hamiltonians and the electron–phonon coupling term. The same general Hamiltonian describes the atom–field interaction in a multi-mode QED cavity [58]. We assume that the QD is occupied by a single electron. Single electron devices that make use of tunnel barriers have been

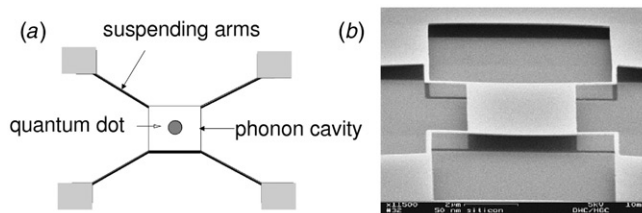


Figure 3. (a) Model quantum dot structure in a free-standing square phonon cavity. (b) Free-standing silicon plate that is 50 nm thick and 4 μm long, produced by the Cornell Nanofabrication Facility.

characterized extensively [59–62]. Thus, for a two-dimensional circular QD of radius R , the undisturbed electronic states are

$$\varphi_\kappa(r, \theta) = \frac{J_{|l|}(\alpha_{lv}(r/R)) \exp[i l \theta]}{\pi^{1/2} R |J_{|l|+1}(\alpha_{lv})|}, \quad (3)$$

with $\kappa \equiv (l, v)$, $l = 0, \pm 1, \pm 2, \dots$ and α_{lv} the v th root of the Bessel function of order $|l|$, $J_{|l|}(\alpha_{lv}, x)$. The corresponding energies are $E_\kappa = (\hbar^2/2m_e)(\alpha_{lv}^2/R^2)$, where m_e is the effective mass of the electron.

The eigenstates of the phonon cavity are obtained through the quantization of its mechanical modes of vibration [57], which are calculated within the classical plate theory [63]. The operators a_α^\dagger and a_α , with $\hat{n}_\alpha = a_\alpha^\dagger a_\alpha$, create and annihilate the phonon modes. Finally, the electron–phonon interaction is written in terms of the matrix elements $V_{\kappa'\alpha\kappa}$ that identify the particular type of interaction between the electrons and the phonons in the cavity. The characteristics of $V_{\kappa'\alpha\kappa}$ depend on the material properties as well as the geometry of the structure. Therefore, it carries information about the symmetries of the nanoelectromechanical system [56, 57]. At low temperatures the more important electron–phonon coupling mechanisms are described by the deformation and piezoelectric potentials, however, only the former is included in (2), because silicon is not a piezoelectric material.

In the present treatment, the basis in which \hat{H} is diagonalized is constructed as the product of the one-electron states $|\phi_\kappa\rangle$ with multi-phonon states $|n_1, n_2, n_3, \dots, n_N\rangle$. Here, $n_\alpha = 0, 1, \dots, n$ denotes the number of phonon quanta in mode α . A total of N distinct phonon modes are considered. A typical basis vector for the compound system is written as

$$|\kappa; \mathbf{n}\rangle = |\phi_\kappa\rangle \prod_{\alpha=1}^N \frac{1}{n_\alpha^{1/2}} (a_\alpha^\dagger)^{n_\alpha} |0\rangle, \quad (4)$$

with $N = 27$ and $n_\alpha \leq 30$ in the following calculations. The convergence of the results has been tested with respect to both the electron and the phonon ensemble sizes. Before the diagonalization of the Hamiltonian is performed, a large ($>10^5$) basis set comprised by states (4) is generated and energy sorted. The diagonalization of \hat{H} is then carried out on a truncated basis of size $\sim 14\,000$. The ensuing coupled electron–phonon eigenstates will serve as basis states for the time propagation of the compound system.

In the remainder we investigate the quantum dynamics of the electronic system coupled to the phonon cavity modes that are described by a thermal field at temperature T . The energy of a multi-mode cavity state $\mathbf{n} \equiv (n_1, n_2, \dots, n_N)$ is $E_{\text{ph}}(\mathbf{n}) = \sum_\alpha (n_\alpha + \frac{1}{2}) \hbar \omega_\alpha$, therefore, the density matrix elements of the phonon ensemble in a thermal configuration are given by

$$\rho_{\mathbf{nn}}^{\text{ph}} = \frac{\exp(-E_{\text{ph}}(\mathbf{n})/k_B T)}{\sum_{\{\mathbf{n}\}} \exp(-E_{\text{ph}}(\mathbf{n})/k_B T)}. \quad (5)$$

In double quantum dot systems, which are analogous to artificial molecules, the decoherence can be observed through the quenching of the oscillating tunnel current between the resonant QDs [5, 6]. In our single quantum dot structure we calculate the time evolution of the electronic angular momentum as it evolves starting from

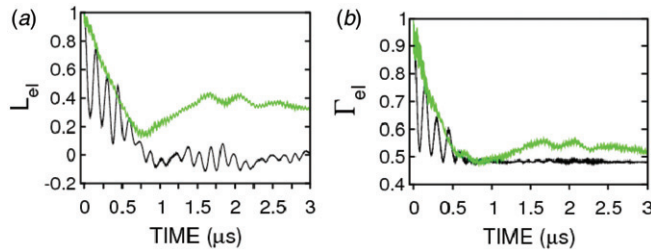


Figure 4. Quantum dynamics of the quantum dot state in the thermal phonon cavity: (a) time evolving electronic average angular momentum L_{el} and (b) decohering process of the electronic state. Black and green curves refer to the QD placed at non-symmetric and symmetric positions in the phonon cavity, respectively. (The colour version of this figure is included in the online version of the journal.)

a well-defined angular momentum state, likewise the atom–field system. Here, we consider the free-standing square phonon cavity, like the one shown in figure 3, with side-length of $1\ \mu\text{m}$ and thickness $50\ \text{nm}$. The QD is $250\ \text{nm}$ in diameter and, therefore, can be treated as a two-dimensional QD. The initial state of the system is the rotational wave-packet $|\Psi(t=0)\rangle = |1, 1\rangle \otimes |\chi_{\text{bath}}\rangle$ that describes a QD in its first excited state ($L_{el} = 1$) in contact with the phonon thermal bath described by equation (5). The temperature of the thermal bath is fixed at $T = 200\ \text{mK}$, which is typical in the study of quantum coherent phenomena.

The position of the quantum dot in the phonon cavity is also important for the system dynamics, due to the interplay between the symmetries of the circular QD states with the square cavity phonon modes. In fact, it has been shown that the spectrum of such suspended nanostructures exhibits a distinct quantum chaotic behaviour depending on the position of the QD inside the phonon cavity [56, 57]. In the following calculations we concentrate on the fully chaotic case (black curve) by placing the QD in the completely nonsymmetric position $(x, y) = (0.650, 0.575)$. In that case the QD-phonon cavity spectrum is characterized by a Gaussian Unitary Ensemble (GUE) of random matrices [64, 65]. For the sake of comparison, if the QD is placed in the centre of the cavity $(x, y) = (0.5, 0.5)$ (green curve) the compound system has a regular dynamics, described by a Poissonian energy level spacing distribution.

Because of the coupling with the phonon cavity, L_{el} is no longer a good quantum number. Figure 4(a) shows the electronic angular momentum $L_{el} = \text{Tr}\{\hat{\rho}_{el}(t)\hat{L}\}$ as it evolves in time coupled with the phonon bath in the cavity. $\hat{\rho}_{el}(t) = \text{Tr}_{\text{ph}}\{\hat{\rho}(t)\}$ is the reduced electronic density matrix and Tr_{ph} designates the trace over phonon states. It is important to observe that the behaviour of L_{el} depends on the position of the QD in the phonon cavity. In both cases the electronic dynamics undergoes a fast phase decoherence (time scale $\tau_1 \sim 0.1\ \text{ns}$) followed by a slower energy dissipation process (time scale $\tau_2 \sim 300\text{--}500\ \text{ns}$). To evaluate more precisely the degree of decoherence in the electronic wavefunction we use the quantity $\Gamma_{el} \equiv \text{Tr}\{\hat{\rho}_{el}^2(t)\}$. At time $t=0$ the electronic system is in the pure state described by $|\Psi(t=0)\rangle$ and $\Gamma_{el} = 1$. The interaction with the phonon cavity is responsible for the decay of Γ_{el} , which stabilizes after τ_2 , indicating that the electronic wavefunction has been partially randomized.

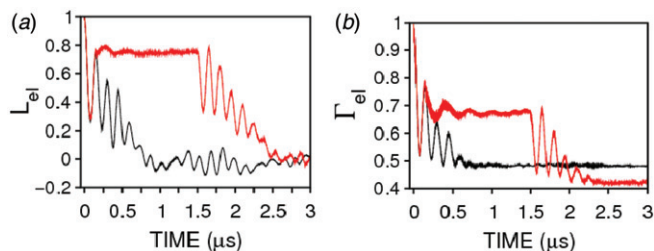


Figure 5. Effect of the coherent quantum control on the dynamics of the electron state in the thermal phonon cavity (red curves), in comparison with freely evolving system (black curves): (a) time-dependent electronic angular momentum L_{el} and (b) decohering process of the electronic state. (The colour version of this figure is included in the online version of the journal.)

Following the original work of Agarwal *et al.* [35], it has been demonstrated that the use of a train of very frequent 2π pulses, both at deterministic and stochastic intervals, can inhibit the tunnelling dynamics in double-well systems as well as in molecule functionalized semiconductor surfaces [28]. Moreover, the technique could be used to steer a wavepacket through discrete quantum states [28]. Here we employ exact calculations and the concept of suspended QD-phonon cavities to demonstrate that the application of successive unitary pulses can also suspend the dynamics and, therefore, the decoherence process in electronic QDs coupled to a thermal bath, without compromise of the underlying quantum coherences. The action of the 2π pulses on the electron–phonon system is realized by the following unitary operator

$$\begin{aligned}\hat{U}^{2\pi} &= \left(\hat{U}^{2\pi}\right)_{el} \otimes \mathbf{I}_{ph} \\ &= (\mathbf{I} - 2|l=1, \nu\rangle\langle l=1, \nu|)_{el} \otimes \mathbf{I}_{ph},\end{aligned}\quad (6)$$

where \mathbf{I}_{ph} is the identity operator. Notice that the π phase is applied to the $l=1$ subspace of the wavepacket, irrespective of the quantum number ν .

The effect of a deterministic train of unitary pulses is demonstrated in figure 5 for the chaotic case, where the dynamics of L_{el} and Γ_{el} (red curves) is presented in comparison with the free dynamics scenario (black curves). Due to the action of the 2π pulses, applied at intervals $\Delta t = 0.9 \text{ ns} \gtrsim \tau_1$, the decoherence and energy dissipation processes are inhibited, because of the dynamical decoupling between the QD and the phonon cavity thermal bath. After the external control is interrupted the QD and the thermal bath resume their original coupled dynamics. We ascribe the additional decoherence produced after the pulse sequence (figure 5(b)) to a side-effect due to the fact that the Zeno limit $\Delta t \ll \tau_1$ is not rigorously attained.

5. Conclusions

We conclude that a simple coherent control scenario based on the repetitive application of frequent phase-kick pulses can efficiently inhibit quantum tunnelling

and decoherence without collapsing the coherent-quantum evolution. These sequences of unitary pulses could be used to achieve coherent control of both bound-to-bound state tunnelling and bound-to-continuum tunnelling processes, in general, so long as the average time-interval between phase-kick pulses is much shorter than the tunnelling time. Furthermore, we conclude that sequences of unitary pulses could also be designed to coherently control electronic decoherence in quantum dots coupled to a thermal bath. Considering the possibility of engineering semiconductor devices at the nano and micro scales, where quantum tunnelling and decoherence phenomena can be tested, it is natural to anticipate considerable experimental interest in examining the proposed coherent control scenario.

Acknowledgements

VSB acknowledges a generous allocation of supercomputer time from the National Energy Research Scientific Computing (NERSC) Center and financial support from Research Corporation, Research Innovation Award #RI0702, a Petroleum Research Fund Award from the American Chemical Society PRF #37789-G6, a junior faculty award from the F. Warren Hellman Family, the National Science Foundation (NSF) Career Program Award CHE #0345984, the NSF Nanoscale Exploratory Research (NER) Award ECS #0404191, the Alfred P. Sloan Fellowship (2005–2006), a Camille Dreyfus Teacher–Scholar Award for 2005, and a Yale Junior Faculty Fellowship in the Natural Sciences (2005–2006). LGC Rego acknowledges allocation of computer time from *Nucleo de Atendimento em Computation de Alto Desempenho* (NACAD-COPPE) in Brazil.

References

- [1] P. Hawrylak, Phys. Rev. Lett. **71** 3347 (1993).
- [2] L.P. Kouwenhoven, D.G. Austing and S. Tarucha, Rep. Prog. Phys. **64** 701 (2001).
- [3] C.W.J. Beenakker, Rev. Mod. Phys. **69** 731 (1997).
- [4] D.P. Vincenzo and D. Loss, Phys. Rev. A **57** 210 (1998).
- [5] J. Gorman, D.G. Hasko and D.A. Williams, Phys. Rev. Lett. **95** 090502 (2005).
- [6] T. Hayashi, T. Fujisawa, H.D. Cheong, *et al.*, Phys. Rev. Lett. **91** 226804 (2003).
- [7] D. Corso, C. Pace, F. Crupi, *et al.*, IEEE Trans. Nanotech. **6** 35 (2007).
- [8] W. Potz, Phys. Rev. Lett. **79** 3262 (1997).
- [9] E. Frishman, M. Shapiro and P. Brumer, J. Chem. Phys. **110** 9 (1999).
- [10] W. Potz, Int. J. Quant. Chem. **85** 398–404 (2001).
- [11] A. Vardi and M. Shapiro, Comments Mod. Phys. **2** D233 (2001).
- [12] B.I. Ivlev, Phys. Rev. A **62** Art. No. 062102 (2000).
- [13] I. Grigorenko, O. Speer and M.E. Garcia, Phys. Rev. B **65** Art. No. 235309 (2002).
- [14] J.M. Villas-Boas, A.O. Govorov and S.E. Ulloa, Phys. Rev. B **69** Art. No. 125342 (2004).
- [15] C. Weiss and T. Jinasundera, Phys. Rev. A **72** Art. No. 053626 (2005).
- [16] A. Matos-Abiague and J. Berakdar, Phys. Rev. B **69** Art. No. 155304 (2004).
- [17] D. Loss and D.P. DiVincenzo, Phys. Rev. A **57** 120 (1998).
- [18] S. Lloyd, Science **261** 1589 (1993).
- [19] D.P. DiVincenzo, Science **269** 255 (1995).
- [20] D.H. Dunlap and V.M. Kenkre, Phys. Rev. B **34** 3625 (1986).

- [21] F. Grossmann, T. Dittrich, P. Jung, *et al.*, Phys. Rev. Lett. **67** 516 (1991).
- [22] M. Holthaus, Phys. Rev. Lett. **69** 351 (1992).
- [23] J. Zak, Phys. Rev. Lett. **71** 2623 (1993).
- [24] X.-G. Zhao, J. Phys. Condens. Matter **6** 2751 (1994).
- [25] S.Ya. Kilin, P.R. Berman and T.M. Maevskaya, Phys. Rev. Lett. **76** 3297 (1996).
- [26] M. Grifoni and P. Hänggi, Phys. Rep. **304** 229 (1998).
- [27] L.G.C. Rego, S.G. Abuabara and V.S. Batista, J. Chem. Phys. **122** 154709 (2005).
- [28] S.G. Abuabara, L.G.C. Rego and V. S. Batista, J. Mod. Opt. **53** 2519 (2006).
- [29] S. Pascazio and M. Namiki, Phys. Rev. A **50** 4582 (1994).
- [30] P. Facchi, S. Tasaki, S. Pascazio, *et al.*, Phys. Rev. A **71** 022302 (2005).
- [31] P. Facchi and S. Pascazio, Phys. Rev. Lett. **89** 080401 (2002).
- [32] K. Koshiro and A. Shimizu, Phys. Rep. **412** 191 (2005).
- [33] M. Maioli and A. Sacchetti, J. Stat. Phys. **119** 516 (2005).
- [34] L.G.C. Rego, S.G. Abuabara and V.S. Batista, Quantum Informat. Computat. **5** 318 (2005).
- [35] G.S. Agarwal, M.O. Scully, H. Walther, Phys. Rev. Lett. **86** 4271 (2001).
- [36] G.S. Agarwal, M.O. Scully and H. Walther, Phys. Rev. A **63** 044101 (2001).
- [37] L. Viola and S. Lloyd, Phys. Rev. A **58** 2733 (1998).
- [38] L. Viola, E. Knill and S. Lloyd, Phys. Rev. Lett. **82** 2417 (1999); *ibid.* **83** 4888 (1999); *ibid.* **85** 3520 (2000).
- [39] M.D. Feit, J.A. Fleck Jr and A. Steiger, J. Comput. Phys. **47** 412 (1982).
- [40] M.D. Feit and J.A. Fleck Jr, J. Chem. Phys. **78** 301 (1983).
- [41] D. Kosloff and R. Kosloff, J. Comput. Phys. **52** 35 (1983).
- [42] Y. Wu and V.S. Batista, J. Chem. Phys. **118** 6720 (2003).
- [43] Y. Wu and V.S. Batista, J. Chem. Phys. **119** 7606 (2003).
- [44] Y. Wu and V.S. Batista, J. Chem. Phys. **121** 1676 (2004).
- [45] X. Chen, Y. Wu and V.S. Batista, J. Chem. Phys. **122** 64102 (2005).
- [46] Y. Wu, M.F. Herman and V.S. Batista, J. Chem. Phys. **122** 114114 (2005).
- [47] Y. Wu and V.S. Batista, J. Chem. Phys. **124** 224305 (2006).
- [48] X. Chen and V.S. Batista, J. Chem. Phys. **125** 124313 (2006).
- [49] R. Bavli and H. Metiu, Phys. Rev. Lett. **69** 1986 (1992).
- [50] E.M. Weig, R.H. Blick, T. Brandes, *et al.*, Phys. Rev. Lett. **92** 046804 (2004).
- [51] E.M. Höhberger, T. Kramer, W. Wegscheider, *et al.*, Appl. Phys. Lett. **82** 4160 (2003).
- [52] A.N. Cleland, *Foundations of Nanomechanics* (Springer-Verlag, Berlin, 2002); R.H. Blick, A. Erbe, L. Pescini, *et al.*, J. Phys. Condens. Matter **14** R905 (2002).
- [53] A.D. Armour, M.P. Blencowe and K.C. Schwab, Phys. Rev. Lett. **88** 148301 (2002).
- [54] A.N. Cleland and M.R. Geller, Phys. Rev. Lett. **93** 070501 (2004).
- [55] T. Brandes, Phys. Rep. **408** 315 (2005).
- [56] L.G.C. Rego, A. Gusso and M.G.E. da Luz J. Phys. A **38** L639 (2005).
- [57] A. Gusso, M.G.E. da Luz, and L.G.C. Rego, Phys. Rev. B **73** 035436 (2006).
- [58] M.O. Scully and M.S. Zubairy, *Quantum Optics* (Cambridge University Press, Cambridge, 2002).
- [59] P.A. Cain, H. Ahmed and D.A. Williams, J. Appl. Phys. **92** 346 (2002).
- [60] A.J. Fergusson, D.G. Hasko, H. Ahmed, *et al.*, Appl. Phys. Lett. **82** 4492 (2003).
- [61] R. Stomp, Y. Miyahara, S. Schaer, *et al.*, Phys. Rev. Lett. **94** 056802 (2005).
- [62] P. Fallahi, A.C. Bleszynski, R.M. Westervelt, *et al.*, Nanoletters **5** 223 (2005).
- [63] K.A. Graff, *Wave Motion in Elastic Solids* (Dover, New York, 1975).
- [64] H.J. Stockmann, *Quantum Chaos: an Introduction* (Cambridge University Press, Cambridge, 1999).
- [65] O. Bohigas, M.J. Giannoni and C. Schmit, Phys. Rev. Lett. **52** 1 (1984).